Properties of the electron-hole liquid in GaP

D. Bimberg* and M. S. Skolnick†
Hochfeld-Magnetlabor des Max-Planck-Instituts für Festkörperforschung, 166X, 38042 Grenoble, France

L. M. Sander
Physics Department, University of Michigan, Ann Arbor, Michigan 48103
(Received 17 July 1978)

An investigation of the luminescence of the polar III-V semiconductor GaP under conditions of high excitation intensity. ($I_{exc} \leq 10$ MW/cm^2) as a function of the excitation intensity, the temperature, and the time after excitation is presented. Evidence is given from time-delayed spectra that at temperatures $T_c \lesssim 45$ K a phase transition from an electron-hole plasma (EHP) to an electron-hole liquid (EHL) occurs. The prominent luminescence band detected in the region of 2.26 eV is proved to be composed of recombination radiation originating from both the EHL and the EHP, a fact that is found to be decisive for a quantitative understanding of the experimental results. The ground-state properties of the EHL are calculated including the effect of the camel's-back-like conduction-band minimum. It is shown to be more important than the electron-phonon interaction correction of the exchange, yielding a ground state energy of 33.3 meV, a binding energy of 14 meV, and a density of 8.6×10^{18} cm^{-3}. An independent determination of E_B from a line-shape fit gives the value 17.5 meV. The high density of states for electrons arising from the camel's back is also shown to strongly influence the ratio of the electron and hole Fermi energies of the EHL, yielding a value of $E_F^h/E_F^e \simeq 4.9$, which should give rise to a strong charging of the drops in GaP. Following a suggestion by Hensel *et al.*, a universal scaling law relating the critical temperature T_c and the low-temperature density n_0 is firmly established for the four best-known materials that exhibit this electronic phase transition and the constant $\beta = \sqrt{n_0}/T_c$ is given as $(7.0 \pm 0.5) \times 10^7$ cm$^{-3/2}$K^{-1}.

I. INTRODUCTION

GaP has several distinctive properties by comparison with other cubic group IV or III-V semiconductors. First, it is one of the most polar[1] of these materials with a Fröhlich coupling constant of $\alpha \simeq 0.22$ for the electrons.[2] Second, the minimum of the conduction band is displaced from the X point of the Brillouin zone and has a very interesting and unusual camel's-back shape.[3-5] As a result of this the longitudinal mass of the electron is highly nonparabolic. It will be shown in this paper that this nonparabolicity has a strong influence on the properties of the electron-hole liquid (EHL) in GaP.

Some evidence for the occurrence of this new electronic phase in GaP at high excitation intensities and low temperatures has recently been presented by several authors.[6-8] These authors observed a new, broad luminescence band, centered at $\simeq 5475$ Å. The line shape of the luminescence line was fitted by all three groups of authors, in a way similar to that employed in the case of Ge,[9] to determine the EHL density and binding energy. Although the input parameters of masses and phonon energies employed in Refs. 6–8 were approximately the same (this is not true for the phonon intensities used), different results were derived from the fits. The values given for the density n range from 6×10^{18} cm^{-3} up to 15.7×10^{18} cm^{-3} and for the binding energy E_B (relative to the free exciton) from 6.2 meV up to 14 meV. The critical temperatures for the transition were given as 20,[6] 40,[7] and 60 K,[8] respectively.

There also exist three different, recent attempts to predict theoretically the $T = 0$ density and binding energy.[8,10,11] The results of the calculations are in better agreement with each other, although the ansatz used differs between the papers. Beni and Rice[10] and Vashishta *et al.*[11] included the electron-phonon coupling in their binding-energy calculation, whereas Hulin *et al.*[8] neglected this aspect and discussed instead the consequences of a sixfold degeneracy of the conduction-band minimum, which would be of importance if the depth of the camel's back were larger than the electron Fermi energy.

We report in this paper the results of excitation-intensity-dependent, time-resolved, and temperature-dependent experiments. Section II describes the experimental arrangement. The *low-temperature* time-delayed spectra given in Sec. III show the reduced gap and the chemical potential to be time independent, thus presenting clear evidence that the new luminescence band indeed arises from an EHL rather than an electron-hole plasma (EHP). It is shown at the high excitation intensities employed that the condensation occurs directly from a hot plasma and not from free excitons. The dominating luminescence band at 2.26 eV is shown there and in Secs. V and VI to be a superposition of an EHL band and an EHP recombination band, their relative contributions to the observed spectrum depending on the actual conditions of excitation and temperature. Recognition of this behavior is decisive for all EHL parameters derived from the experiment. Calculations of the ground-state energy, the density, and the line shape are presented in Sec. IV after making a careful assessment of the conduction- and valence-band parameters and of the intensities of the phonons that couple to the EHL. We show that the camel's back in the conduction band strongly changes the properties of the EHL as compared with those expected for a simple parabolic band. The density and ground-state energy are strongly enhanced. The electron Fermi energy is reduced by more than 40% whilst the hole Fermi energy is increased, giving rise to a large ratio (4.9) between the hole and electron Fermi energies, which in turn should give rise to a strong surface charge of the EHL. These changes occur because of the high density of states at the bottom of the conduction band arising from the presence of the camel's back. The sixfold degeneracy of the absolute conduction-band minimum is of no direct significance since the electron Fermi energy is larger than the depth of the camel's back.

A theoretical line shape derived on the basis of these calculations is found in Sec. V to describe well the shape of the experimentally observed EHL band without using any adjustable fitting parameters. The large EHL binding energy of 17.5± 3 meV derived from this comparison is found to be in good agreement with the theoretical binding energy of 14 meV calculated in Sec. IV. This binding energy is larger than any value previously reported.

High-temperature time-delayed and intensity-dependent spectra are discussed in Sec. VI. Whereas at low bath temperatures ($T_{\mathrm{bath}} \sim 1.8$ K) with increasing time-delay bound-exciton luminescence is more important on the high-energy side of the line, at temperatures around 30 K free-exciton lines are observed at long delay times. A value of the critical temperature T_c of ~45 K is estimated from these experiments. This value of T_c and the density $n_0 = 8.6 \times 10^{18}\ \mathrm{cm}^{-3}$ derived in Sec. IV are shown to obey well a universal scaling rule connecting these two parameters.

II. EXPERIMENTAL

The luminescence of pure n-type GaP was excited by a 1-MW, 337-nm Lambda Physik N_2 laser. The exciting pulses had a half-width of ~2 nsec. The luminescence was detected and analyzed with a fast photomultiplier and a PAR 160 boxcar integrator. The time resolution of the total system was ~15 nsec. For $T \leqslant 4.2$ K, the spectra were taken with the sample directly immersed in liquid He and at $T \geqslant 4.2$ K with a He-gas flow cryostat.

The excellent samples used here were grown by liquid-phase epitaxy. Nitrogen and sulphur impurities were present at concentrations of $<10^{15}$ cm^{-3}. The crystals were kindly donated by Dr. D. R. Wight of the Services Electronic Research Laboratory, Baldock, U. K., and by Dr. Weyrich, Siemens Forschungslaboratorien, München, Germany.

III. LOW-TEMPERATURE TIME-DEPENDENT RESULTS

In this section low-temperature time-delayed spectra and decay times are presented in order to establish firmly the existence of the EHL in GaP. The generation and annihilation processes of the EHL are discussed and decay times are given.

Figure 1 shows in a three-dimensional diagram the time evolution of the EHL spectra at 1.8 K. The spectra are normalized to the same height. Their true relative intensities can be derived from Fig. 2. All spectra were taken at the same, highest excitation intensity possible, just before the surface of the crystal was damaged by overheating. This effect (which is probably due to the imperfect sample surface having a very high absorption coefficient) limited the maximum excitation. The zero on the time scale is set to the maximum of the exciting N_2-laser pulse. The shape of such a pulse, as given by the detection system

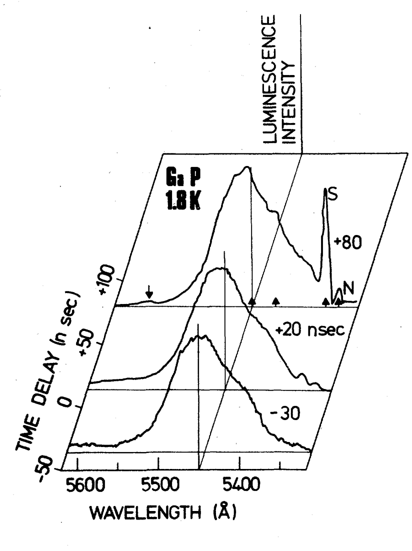

FIG. 1. Low-temperature luminescence spectra taken at an excitation intensity of $\simeq 10\ \mathrm{MW/cm}^2$ at three different delays relative to the peak of the exciting N_2-laser pulse. The arrows in the 80-nsec spectrum indicate the wavelengths at which impurity-induced features occur at this delay. N and S refer to the N- and S-bound excitons, respectively.

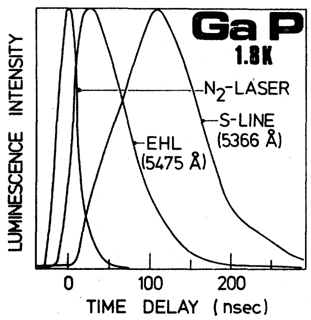

FIG. 2. Intensity as a function of time for the exciting N_2-laser pulse, the peak of the EHL band, and the S-(Te-) bound exciton line. The width of the N_2-laser pulse here was caused by charging of the multiplier, which occurred if the exciting pulse was measured under the same conditions as the signal.

is displayed in Fig. 2. Even at the maximum "negative" delay of 30 nsec at which spectra could be taken the typical EHL line shape is found. At this delay no free excitons and only negligibly small bound exciton lines are observed.

The time evolution of the spectra indicate that the EHL condenses extremely quickly from an EHP, without free excitons being created. The high-energy side of the EHL band at −30 nsec is somewhat broadened relative to the spectra closer to zero delay. This broadening can be attributed to the recombination radiation from a residual plasma, which does not disappear completely at any delay time. The lineshape is exactly the same between −20 and +20 nsec. This is characteristic behavior of an EHL with fixed reduced gap and Fermi energy (density) as opposed to an EHP where the density decreases with time.[2,9] At larger positive delays (i.e., at longer times after the exciting pulse) the low-energy side still remains the same. However, on the high-energy side bound-exciton lines appear. These impurity lines grow rapidly with increasing delay and finally dominate the spectra at very long delay times. They are due to the recombination of excitons bound to nitrogen[12] and sulphur (or tellurium).[13] It will be shown in Sec. IV that the density inside the EHL in GaP is of the order of 10^{19} cm^3 and so Auger processes dominate the recombination. Auger electrons and holes are ejected from the EHL (and the EHP, of course) and captured by impurities (at 1.8 K) after the excitation is switched off and the EHP density becomes too low for further EHL production.

Figure 2 shows the normalized intensities of the exciting N_2 laser, the EHL, and the sulphur (tellurium) bound-exciton lines on a time axis. It can be seen that the EHL reaches its maximum 20 nsec after the N_2-laser peak. The bound-exciton line shows a rather slow increase and only reaches its maximum after the EHL luminescence has decreased to $\simeq 20\%$ of its peak value. It is apparently fed from the decay of the EHL. It should be noted that the EHL line shape at +20-nsec delay, where it has its maximum intensity, is not influenced significantly by any residual bound-exciton features. Therefore we do not need to perform any corrections for bound excitons in order to compare with a theoretical line shape. The EHL band is the sum of the TA(X), LA(X), and TO(X) phonon replica of the recombination radiation of the EHL. The main peak at 5475 Å is due to the LA(X) replica. The weak shoulder on the high energy side at 5416 Å has been attributed to the TA(X) replica.[6,7] However, the energy difference between the two is $\simeq 24.6$ meV, 6.4 meV larger than the difference between the well-known phonon energies.[13,14] Since the high-energy shoulder, as pointed out earlier, is time dependent and is also found to be somewhat excitation-intensity dependent, one can conclude that it probably arises from a lower density plasma, rather than from the TA(X) replica of the EHL. It was also found that the lifetime at 5416 Å was $\simeq 20\%$ longer than that at the peak ($\tau_{peak} = 37 \pm 2$ nsec), which is another indication for the presence of a low density plasma (or of long-lived impurity lines). In contrast to this the lifetime on the low-energy side at 5510 Å was found to be the same as the lifetime at the peak. This is very similar to the results which were recently found for cubic SiC.[2]

The line shape at 20-nsec delay will be compared in Sec. V with the results of the calculations presented in Sec. IV and more evidence for the presence of an EHP on the high-energy side of the 2.26-eV line presented.

IV. CALCULATION OF THE EHL BINDING ENERGY AND OF THE LUMINESCENCE LINE SHAPE

In this section the ground-state energy and the luminescence line shape of the EHL are calculated. These calculations are compared in Sec. V with the experimental results and good agreement is found.

Our ansatz contrasts with the methods used in some recent publications,[6,7] where the line shape was calculated, using the density and/or the ratio of the phonon replicas as adjustable parameters. In this paper improved band-structure parameters are used and the peculiar camel's-back shape of the conduction band is taken into account. The exact parameters of the camel's back are controversial. However, the two most probable sets of parameters yield almost the same density of states and therefore the same EHL properties as will be seen later.

A. Conduction band of GaP

GaP has a similar band structure to Si. In Si the minima of the conduction band are in the ⟨001⟩ directions, displaced by approximately $0.15k_{max}$ from the edge of the Brillouin zone at the X point. The conduction bands are degenerate at the X point. By going from Si to GaP the inversion symmetry is removed. Consequently the degenerate bands at the X point are split into a higher-lying X_3 band and a lower-lying X_1 band. The energy difference $\Delta = E(X_3) - E(X_1)$ is 355 meV.[15] The absence of inversion symmetry can introduce a camel's-back-like structure in the conduction band,[4,5] similar to the case of the valence bands in Te.[16] This possibility was first noted by Pollak *et al.*[4] Lawaetz[5] recently investigated theoretically the conditions under which the camel's back would be present. He[5] obtained values for its characteristic parameters, the depth ΔE and the displacement of the minimum k_{min} from the X point, as $\Delta E = 1.4$ meV and $k_{min} = 0.07k_{max}$ on the basis of $\vec{k}\cdot\vec{p}$ perturbation theory and a comparison with Si. Lawaetz[5] also calculated a theoretical value of $\Delta = 420$ meV, which is 65 meV larger than the experimentally known value. An example of an energy against wave vector dispersion relation for a camel's-back band is illustrated in Fig. 3, curve 1.

Hensel and Kane[17] have criticized the perturbation-theory approach and proposed instead that a pseudopotential method should be used. However, they agree that the critical parameter (in Lawaetz's notation Δ/Δ_0, where Δ_0 is the energy difference between the Si conduction-band minimum and the next higher conduction band) is close to 1, the critical value. This means that one expects in any case with or without camel's back a highly nonparabolic, flat minimum ($m_l \to \infty$).

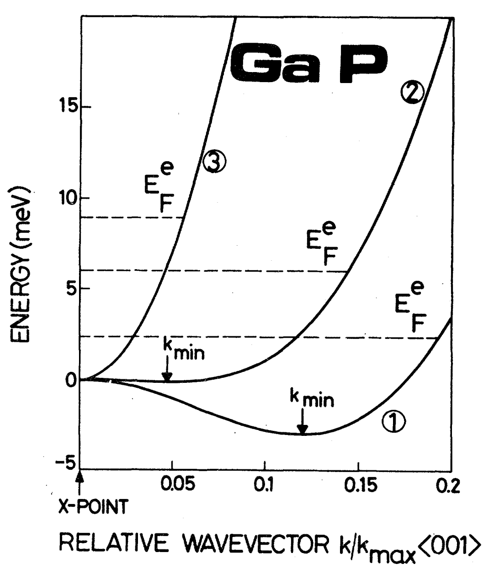

FIG. 3. Dispersion of the conduction band of GaP at the X point of the Brillouin zone. k_{min} indicates the minimum of the band and E_F^e gives the position of the electron Fermi level. The parameters are (1) $m_{in} = 7.22m_0$, $m_{out} = 2.2m_0$, $k_{min} = 0.12k_{max}$ (set 2 of Table I); (2) $m_{in} = 25m_0$, $m_{out} = 1.8m_0$, $k_{min} = 0.047k_{max}$ (set 1 of Table I); (3) $m_{in} = m_{out} = 1.8m_0$, no camel's back.

Direct experimental evidence for the presence of a shallow camel's back and extremely high nonparabolicity is available. The first indication dates back to the absorption experiments of Dean and Thomas[18] and Pikhtin and Yas'kov,[19] who obtained fine structure in their spectra, which could not be explained within the framework of the usual exciton theory. More recently, Dean and Herbert[3] have reinterpreted phonon satellites of the fundamental luminescence lines of excitons bound to neutral acceptors. They attributed these satellites to momentum-conserving g-type intervalley scattering in the conduction band. The position k_0 of the conduction-band minimum in k space was derived to be $\Delta k \simeq 0.047k_{max}$ from the X point, where $k_{max} = 2\pi/a$ with the lattice constant $a = 5.449$ Å.[20]

Still more recently, Humphreys *et al.*[21] using wavelength modulated absorption spectroscopy under uniaxial stress were able to resolve clearly the exciton fine structure of Dean and Thomas.[18] For the exciton energy bands they deduced the energy separation of the absolute minima of the camel's back and the energy of the saddle point at the X point to be 2.4 and 2.6 meV for the two exciton ground states, in qualitative agreement with lower-resolution results of Capizzi *et al.*[22] Altarelli *et al.*[23] have calculated the dispersion of the exciton band as compared with the conduction band.

Using these calculations one obtains a depth of $\Delta E = 3.1$ meV. Very similar conclusions have been drawn by Kopylov and Pikhtin[24] from an analysis of the infrared absorption spectra of donors, a value of $\Delta E = 3$ meV being deduced.

The dispersion relation in the longitudinal direction for a band with a camel's back can be written in the form

$$E(k) = Ak^2 - [(\Delta/2)^2 + \Delta_0 Ak^2]^{1/2}\,, \qquad (1)$$

neglecting higher-order terms.

The interpretation of the quantities Δ and Δ_0 has already been discussed. Δ_0 is not known in GaP. For $k \to \infty$ one obtains

$$E(k) \simeq Ak^2 = \hbar^2 k^2/2m_{out}\,, \qquad (2)$$

and so

$$A = \hbar^2/2m_{out}\,, \qquad (3)$$

where m_{out} is the longitudinal mass at energies distant from the conduction-band minimum. The value of this outer mass was recently estimated by Dean *et al.*[25] and Carter *et al.*[26] from some older Raman data of Manchon and Dean.[27] Using $m_t = 0.275m_0$,[26] and $m_l/m_t \simeq 6.7$,[26] one obtains $m_{\text{out}} = 1.8m_0$. An $m_t = 0.254m_0$ would yield the value $m_l/m_t = 9.5$ and $m_{\text{cut}} = 2.41m_0$ from a similar analysis. The $1S(E)$ donor states involved in these Raman transitions are about 54 meV deep. Therefore a somewhat more sophisticated discussion should take into account an energy-dependent dielectric constant, since $E_B[1S(E)] \simeq \hbar\omega_{\text{LO}}$, the longitudinal-optical-phonon frequency ($\hbar\omega_{\text{LO}} = 50.1$ meV).[27] The mass m_{in} *exactly* at the bottom of the camel's back was not determined experimentally. It can be calculated using the first and second derivatives of the dispersion formula (1). From the first derivative of (1) one obtains a condition which determines Δ_0

$$Ak_{\min}^2 = \tfrac{1}{4}\Delta_0[1 - (\Delta/\Delta_0)^2]\,. \tag{4}$$

The second derivative of (1) gives an expression for m_{in}:

$$m_{\text{in}} = m_{\text{out}}/[1 - (\Delta/\Delta_0)^2]\,. \tag{5}$$

Using the values (set 1) $m_{\text{out}} = 1.8m_0$, $\Delta = 355.5$ meV, and $k_{\min} = 0.047k_{\max}$ just mentioned, one gets $\Delta_0 = 368$ meV and $m_{\text{in}} = 27m_0$. It should be noted that the longitudinal mass m_{in} is always larger than m_{out} if one has a camel's back. The value m_{in} derived here can be compared with some recent experimental results. Cyclotron resonance experiments by Leotin *et al.*[28] and Suzuki and Miura,[29] and infrared-absorption experiments by Carter *et al.*[26] give some kind of average value for m_{in}. The cyclotron resonance experiments of Leotin *et al.*[28] yield a value of $m_l = 5^{+2.5}_{-1.5}m_0$ as an average over energies of up to 10 meV above the bottom of the conduction band. Carter *et al.*[26] find $m_l = 7.25m_0$ from an investigation of still shallower excited donor states. All of these values are smaller than the m_{in} calculated using the parameters of Ref. 5. Finally the depth of the camel's back can be determined from Eq. (1) and set 1 to be 0.1 meV, a surprisingly small energy. This value of ΔE is in clear contradiction with the result $\Delta E = 3$ meV of the wavelength-modulated piezoabsorption[21–23] and the ir absorption[24] discussed above.

Combining the value $\Delta E = 3$ meV with $\Delta = 355.5$ meV and a value of $m_{\text{in}} = 7.25m_0$ in agreement with the results of Carter *et al.*[26] and the cyclotron resonance data, we have a second "complete" set of parameters that determines the dispersion of the longitudinal energy. This second set is rather different from the first one as far as the depth

TABLE I. GaP band-structure parameters used in this paper and in Refs. 6–8. The masses are polaron masses.

Parameter	This paper set 1	set 2	Refs. 6–8 set 3
m_{out}	$1.8m_0$ [a]	$2.2m_0$ [b]	$1.7m_0$ [c]
m_{in}	$25m_0$ [b]	$7.25m_0$ [a]	$1.7m_0$
$k_{\min}$	$0.047k_{\max}$ [d]	$0.12k_{\max}$ [b]	0
ϵ_0	11.02 [e]		11.02 [e]
m_t	$0.254m_0$ [a]		$0.19m_0$ [c]
γ_1	4.05 [f]		4.7 [g]
γ_2	0.489 [f]		1.3 [g]
γ_3	1.247 [f]		1.56 [g]
$\hbar\omega$ (TA)	13.1 meV [h]		12.8 meV [i]
$\hbar\omega$ (LA)	31.5 meV [h]		31.3 meV [i]
$\hbar\omega$ (TO)	45.4 meV [h]		46.5 meV [i]
I(TA):I(LA):I(TO)	0.34:1:0.4 [j]		0.52:1:0.38 [k] (Ref. 6)
			0.52:1:0.88 (Ref. 7)
			0.36:1:0.27 [k] (Ref. 8)

[a] Reference 26.
[b] Calculated in this paper on the basis of published data (see text).
[c] Reference 15.
[d] Reference 5.
[e] Reference 30.
[f] Reference 34.
[g] Reference 64.
[h] Reference 40.
[i] Reference 18.
[j] Figure 1 of Ref. 14.
[k] Reference 39.

and location of minimum in k space is concerned. A $k_0 = 0.12k_{max}$ is calculated from the second set and yields a value of $m_{out} = 2.2m_0$ in agreement with the Raman data discussed above. Assuming an $m_{in} = 5m_0$ we would still get $k_0 = 0.10k_{max}$. The latter values would yield almost the same density of states for electrons as the former one. Both values would force a reinterpretation of the satellites of the acceptor bound excitons of Ref. 5. On the other hand, they yield approximately the experimentally determined binding energy of the E-donor states of Manchon and Dean.[27] The two different sets of conduction band parameters are collected together with the parameters of the valence band and the phonons in Table I and compared with the set of parameters used in Refs. 6–8 (set 3). Figure 3 shows a comparison of the energy dispersion for the two different sets of camel's-back parameters with a parabolic dispersion curve calculated for $m_{out} = 1.8m_0$. The electron Fermi energies of an EHL calculated in a way described later are given by horizontal dashed lines. The two energy dispersions calculated for the different sets of camel's-back parameters shown in Fig. 3 are clearly different. However, it is not in fact the value of ΔE, the depth of the camel's back, or its location in k space, but the large and highly anisotropic mass at the bottom of the conduction band and the spread of an almost "flat" part of the band over a range of more than 10% of the Brillouin zone that are highly important for the properties of an EHL. They strongly increase the electron density of states at the bottom of the band and therefore reduce the electron Fermi energy. This is nicely illustrated in Fig. 4, which contrasts the density of states for a conduction band calculated with the above three sets of parameters. It is not too surprising that the density of states for the two sets of camel's-back parameters are rather close to each other and about one order of magnitude higher than the density of states for the parabolic band of Fig. 3. We will see later that there is also almost no difference between the characteristic properties of an EHL for the two different sets of camel's-back parameters. However, there is a large difference as compared to the case without camel's back.

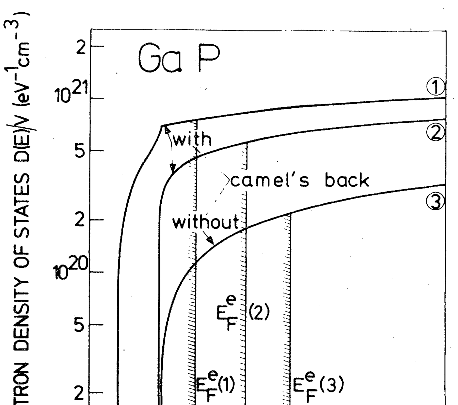

FIG. 4. Density of states of the conduction band of GaP at the X point of the Brillouin zone. E_F^e gives the position of the electron Fermi level. The parameters are (1) $m_{in} = 7.2m_0$, $m_{out} = 2.2m_0$, $k_{min} = 0.12k_{max}$ (set 2 of Table II); (2) $m_{in} = 25m_0$, $m_{out} = 1.8m_0$, $k_{min} = 0.047k_{max}$ (set 1 of Table I); (3) $m_{in} = m_{out} = 1.8m_0$, no camel's back. The zero of energy is taken at the X point.

Carter *et al.*[26] also find some indication for a small k-dependence of the transverse mass m_t from the Zeeman splitting of different p-like donor states. A mean value of $m_t = 0.254m_0$ of the values given by Carter *et al.* is used here since the scatter of the various values is only ~10% of the mean value.

B. Valence band

The spread of the values of the valence band parameters given in the literature is less than for those of the conduction band. Street and Senske[31,32] have recently derived a set of Luttinger parameters $\gamma_{1,2,3}$ from a comparison of acceptor excited state spectra with calculations of Baldereschi and Lipari.[33] An improved fit[34] has yielded somewhat corrected values (see Table I). These new values will be used here since they give almost the same cyclotron resonance mass values for $\vec{H}\|\langle 111\rangle$ of $m_{hh} = 0.545m_0$, $m_{lh} = 0.159m_0$ as Leotin *et al.*[35] found in their experiments for this field direction. The kinetic energy of the holes was calculated employing as density-of-states mass m_d the theoretical cyclotron resonance mass for $\vec{H}\|\langle 110\rangle$,[36]

$$\left(\frac{m_{cr}}{m_0}\right)^{-1} = \{\gamma_1 \pm [2(\gamma_2^2+\gamma_3^2)]^{1/2}\} \times \left(1 \mp \frac{9(\gamma_3^2-\gamma_2^2)(-\frac{5}{9} - 2\cos^2\theta + 3\cos^4\theta)}{16[2(\gamma_2^2+\gamma_3^2)]^{1/2}\{\gamma_1 \pm [2(\gamma_2^2+\gamma_3^2)]^{1/2}\}}\right), \quad (6)$$

where $\theta = 90°$ is the angle in the (110) plane between the magnetic field and the $\langle 100\rangle$ direction. This angular average gives $m_{hh} = 0.516m_0$ [see Eq. (10)]. It should be noted that a partial neglect of the warping[10,37] leads to a rather different value for the heavy hole mass, which largely determines the hole Fermi energy.

C. Phonons

The recombination of an electron from close to the X point with a hole from the Γ point can take place only with the participation of a momentum-conserving phonon. Auvergne *et al.*[38] have recently rediscussed the selection rules for such phonons. According to their arguments the LA-phonon replica should dominate free-carrier absorption or emission. The TA-, TO-, and LO-assisted transitions should be weaker, Interband absorption[18,19] and free-exciton emission[14,39] experiments show indeed that LA-assisted transitions are stronger than TA- and TO-assisted transitions. However, no one-phonon LO-assisted transitions are observed in either type of experiments, so it might be worthwhile to reexamine the selection rules theoretically. For the analysis of the EHL line shape, the LO-assisted transitions will be neglected, in accordance with the experimental observations of the interband and free-exciton measurements. Dean *et al.*[40] determined the energies of the three-momentum-conserving phonons with high precision from bound-exciton recombination. They obtain

$$E_{TA}=13.1 \text{ meV}, \tag{7a}$$

$$E_{LA}=31.5 \text{ meV}, \tag{7b}$$

$$E_{TO}=45.4 \text{ meV}. \tag{7c}$$

These values are in good agreement with the values derived by Mobsby *et al.*[14] from free-exciton emission.

From Fig. 1 of the luminescence spectra of Mobsby et al.[14] we have determined the ratios

$$I(\text{TO}):I(\text{LA}):I(\text{TA})=0.40:1:0.34, \tag{8}$$

which are in excellent agreement with the older absorption data[18] $[I(\text{TO}):I(\text{LA}):I(\text{TA})=0.39:1:0.27]$. The first set of intensity ratios will be used in our calculations. It should be mentioned that the intensity ratios 0.38 : 1 : 0.52 which were used by Maaref *et al.*[6] and the ratios 0.88 : 1 : 0.53 employed by Shah *et al.*[7] to fit their data are not consistent with available experimental results on free excitons. There is no reason to suppose that the selection rules for *allowed* transitions would be significantly changed on going from the free-exciton case (at, e.g., 25 K) to the EHL since the range of $\vec{k}$ vectors involved in the two cases is very similar. The experimental finding by Thomas and Capizzi[41] that the ratio I_{LA}/I_{TO} is identical for the free exciton and the EHL in Ge agrees with this argument.

The sum of the electron and hole Fermi energies in the EHL is much smaller than the energy range in which, e.g., absorption experiments[18,19] were performed and in which a good theoretical fit was achieved with the above intensity ratios. The TA and TO phonons do not show any appreciable energy dispersion in the k range that is of interest here.[42] This range of interest covers up to $\simeq 23\%$ of the Brillouin zone away from the X points, since the Fermi wave vector of the electrons is found to be $\simeq 0.82k_{max}$ (see Sec. IV D) and the heavy hole wave vector is $\simeq 0.05k_{max}$. The LA-phonon energy decreases between $k_{max}([001])$ and $0.75k_{max}([001])$ by 3.8 meV.[42] LA phonons with wave vectors $0.77k_{max} < k < 0.87k_{max}$ will be involved in the recombination between electrons and holes that come from regions close to their respective Fermi levels. The slightly reduced energy of these phonons relative to the X-point phonons leads to a broadening of the LA EHL line. This inhomogeneous broadening also depends on the phonon density of states. For simplicity it will not be taken into account in the calculation of the line shape in Sec. IV E. It is quite clear that this effect which will slightly *reduce* the separation of the LA and TA EHL components cannot explain the discrepancy of 6.5 meV between the experimental spacing of the high-energy shoulder and the peak of the luminescence line and that of the known LA-TA separation as was discussed in Sec. III. In fact, the dispersion of the LA phonon increases the discrepancy to ~8.5 meV.

D. Ground state of the EHL

The total energy of the EHL has been numerically determined as a function of the density where

$$E_{tot}=E^e_{kin}+E^h_{kin}+E_{exch}+E_{cor}. \tag{9}$$

The kinetic energies of the electrons E^e_{kin} and of the holes E^h_{kin} were calculated in a straightforward way. The hole kinetic energy is given by[43]

$$E^h_{kin}=(\hbar^2/2m_{hh})\tfrac{3}{5}\,[3\pi^2 n/(1+\Gamma^{3/2})]^{2/3}, \tag{10}$$

with $\Gamma=m_{lh}/m_{hh}$.

The electron kinetic energy was numerically evaluated by means of an integral over the actual density of states $D(E)$

$$E^e_{kin}=\int_0^{E^e_F}\frac{ED(E)}{V}\,dE\Big/\int_0^{E^e_F}\frac{D(E)}{V}\,dE. \tag{11}$$

E^e_F is the Fermi energy of the electrons and V is the volume. E^e_F is, of course, no longer proportional to $n^{2/3}$ as in the case of a parabolic dispersion relation. The masses used here as input parameters were discussed in the preceding sections.

A calculation of the exchange and correlation energy in GaP would be difficult because of the complicated band structure. However, Störmer *et al.*[44] have found that the change of the density and the binding energy of the EHL in Ge in magnetic fields up to 20 T could be well understood in terms of the calculable field dependence of the kinetic energy whilst taking the sum of $E_{exch}+E_{cor}$

as a constant independent of the magnetic field, although the exchange alone depends on field.[45] This constancy of the total Coulomb energy of a two component plasma is remarkable. We propose that it results from one aspect of the following semiempirical scaling rule[46]: the Coulomb energy in units of the exciton Rydberg is a *universal function* of $r_s = 1/(\frac{4}{3}\pi n)^{1/3} a_x$, where a_x is the exciton radius. This "rule" can be easily checked against calculations for *different* materials[47] (Si, Ge, strained and unstrained). The scatter in the values of the "universal function" is about ± 10%. The known values of $E_{\text{exch}} + E_{\text{cor}}$ for Ge, as given by Vashishta *et al.*,[47] were therefore used here suitably scaled.

It may be that scaling of this sort can be justified by noting that the Coulomb energy is dominated by the plasmon pole in the response function[48] and is thus more or less independent of band structure or magnetic field. In any case, we think that the scaling argument is as reliable as any other method to find E_{tot} in GaP, and we have used it in our calculations.

GaP is a polar material. We may expect that the electron phonon coupling will enhance the binding energy.[48,49] Much of the effect has already been taken into account since we use the low-frequency dielectric constant $\epsilon_0 = 11.02$. This "ϵ_0 approximation" is reasonably accurate provided E_F^e, $E_F^h \ll \hbar\omega_{\text{LO}}$. Since $\hbar\omega_{\text{LO}} \simeq 50$ meV in GaP, we are within this limit. The next correction—to the exchange energy—is given by Keldysh and Silin[49]:

$$\Delta E = -\frac{3}{12\pi}(1 + 3^{-1/3})(3\pi^2)^{1/3} e^2 n^{1/3} \frac{(\epsilon_0 - \epsilon_\infty)}{\epsilon_0 \epsilon_\infty} = -1.17 \times 10^{-6} n^{1/3} \text{ meV}. \tag{12}$$

Equation (12) has taken the band structure into account by using one hole band and three isotropic electron bands. A more precise calculation using, e.g., the camel's back would be difficult. The effect of (12) is, however, already quite small: E_{tot} is increased by 8% and the density n increases by 3%. Therefore no change within about a 1% limit is expected from a more detailed calculation of the exchange correction for this material.

In Table II our most important results are collected together and compared with those of other authors. We find a somewhat larger ground-state energy for the set 3 of parameters in Table I than Hulin *et al.*[6] who obtained $E_G = 20$ meV with a density of 5×10^{18} cm^{-3} using the same parameters since different values for $E_{\text{exch}} + E_{\text{cor}}$ and a different averaging of the hole mass were employed by them.

From a comparison of rows 3 and 5 it can be seen that the introduction of the correct larger transverse electron mass m_t and of the slightly larger hole mass increases appreciably the binding energy and the density without strongly changing the ratio of the electron and hole Fermi energies. Adding now the camel's back and the electron-phonon interaction (EPI) and comparing rows 1, 2, and 3 the following points should be noticed:

(i) There is only a small difference between

TABLE II. Comparison of the results of the present calculations using the parameters given in Refs. 6–8 (row 5), our best choice of parameters with camel's back and EPI (rows 1 and 2), and without camel's back and EPI (row 3) are compared with the results of Beni and Rice (Ref. 10) and Vashishta *et al.* (Ref. 11 taken from Ref. 7). E_G is the ground state energy and E_F is the Fermi energy, where the index e denotes electrons and the index h denotes holes.

Input parameters	Ground-state energy E_G (meV)	Fermi energies E_F^e	E_F^h	$\sum_{e,h} E_F$	Density n (10^{18} cm^{-3})
Our best choice					
(a) set 2 of Table I	33.3	5.4	26.7	32.1	8.6
(b) set 1 of Table I	33.2	6.0	25.8	31.8	8.2
Our best choice (set 2 of Table I) without camel's back and EPI	26.3	9.0	17.0	26.0	4.4
Our best choice with camel's back without EPI	30.9	5.3	26.2	31.5	8.4
As used in Refs. 6–8 (set 3 of Table I)	23.2	11.4	15.9	27.3	4.1
Beni and Rice					
without EPI	26.5			29.9	5.0
with EPI	(29.9)			(39.3)	(7.1)
Vashishta *et al.*	27.6				6.5

the results for the two sets of camel's backs, although the dispersion curves (Fig. 3) are quite different. This demonstrates clearly that, as stated earlier, the integrated density of states is the important quantity for the EHL parameters.

(ii) The density in the drop and the groundstate energy are increased by 95% and 27% respectively, mainly owing to the camel's back. A much higher ground-state energy E_G and density are found as compared to those given in the earlier work. Using a theoretical binding energy of 19.5 meV for the exciton ground state[50]—in agreement with recent experimental values of Sturge *et al.*[32] and Bindemann *et al.*[51]—one derives from our results given in Table II at large EHL binding energy of 14 meV, a value that agrees very well with experimental results (see Sec. V).

(iii) The effect of the camel's back on the Fermi energies of the electrons and holes is still more important than the effect on the binding energy and the density. The sum of the Fermi energies increases by (only) 23%. However, the ratio of E_F^h/E_F^e changes drastically from 1.9 to 4.9. It will be seen that this has a large effect on the theoretical line shape at zero temperature, which will be calculated in Sec. IV E. The large difference of electron and hole Fermi energies will also influence strongly the charge of the drop.[52-56]

The sign of the charge depends on the difference of the total chemical potentials for electrons and holes, which govern the evaporation processes on the surface of a drop. There are two contributions to the total chemical potential, one from the bulk and another from the dipole layer on the surface. The difference in the bulk chemical potentials of electrons and holes is to a good approximation equal to the difference of their respective Fermi energies. This difference is more than one order of magnitude larger in GaP than, e.g., in Ge, where explicit calculations have been made.[52-55] The dipole layer on the surface is a result of the difference between the radial charge density distribution of the electrons and the holes. It was recently shown by Kalia *et al.*[55] for Ge that the contribution of the surface dipole layer to the total chemical potential is much smaller than the difference ($\simeq 1.4$ meV) between the Fermi energies. The sign (and partly the size) of the charge of the drop is therefore mainly a function of the difference of the Fermi energies. Assuming the same is true for GaP the drops should be strongly negatively charged in this material.

In conclusion, it can be stated that a camel's-back structure in the conduction band of GaP has a large influence on the ground-state properties of an EHL due to the high density of states at the bottom of the camel's back. This effect in GaP is much larger than the polaron correction to the exchange term [Eq. (12)].

E. Calculation of the line shape

Theoretical spectra have been calculated as a sum of the three appropriately displaced phonon replica of different intensities. The phonon energies and intensities were discussed in Sec. IV C. The line shape of each (one-phonon) band was calculated as a convolution integral over the correct electron and hole densities of states using the parameters discussed above for the theoretically derived density.

In Fig. 5(a) the theoretical line shapes of the one-phonon EHL lines calculated with and without camel's back, using the parameters given in set 1 of Table I, are compared with one another for low temperature ($T = 1$ K).

The line shape calculated with a camel's-back dispersion is strongly asymmetric. It mainly displays the hole density of states, whereas that

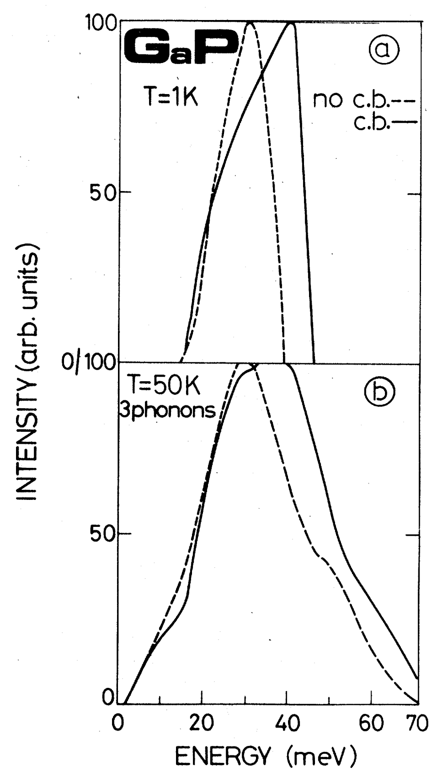

FIG. 5. Different theoretical EHL line shapes calculated for a parabolic conduction band (solid line; $m_{\text{in}} = m_{\text{out}} = 2.2\, m_0$) and a conduction band with a camel's back (dotted line; $m_{\text{in}} = 7.22\, m_0$, $m_{\text{out}} = 2.2\, m_0$, $k_{\text{min}} = 0.12\, k_{\text{max}}$). The valence-band parameters used are given in Table I, column 1 and the Fermi energies were calculated in Sec. IV D. (a) one-phonon line at $T = 1$ K. (b) Line composed of LA, TA, and TO components (the energies and intensities of the phonons are discussed in Sec. IV C) at T 50 K.

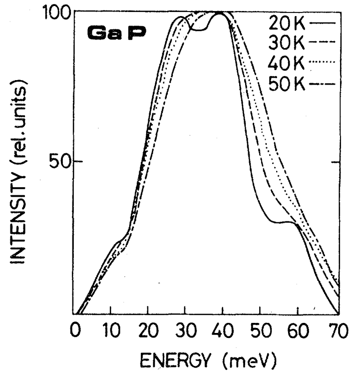

FIG. 6. EHL line shapes calculated for a conduction band with a camel's back for the same parameters as in Fig. 5(b) but for different $T = 20$, 30, 40, and 50 K. The low-energy sides always coincide for the different temperatures. The high-energy shoulder due to the TA phonon disappears with increasing temperature at $\simeq 30$ K.

calculated without the camel's back has the conventional form obtained for parabolic bands. The superposition of the three-phonon replica at a temperature of, e.g., 50 K (or in the presence of any other kind of broadening mechanism) partially smears out the asymmetry, as shown in Fig. 5(b). Despite the high temperature there remains some difference in the shapes of Fig. 5(b) mainly at the top of the line, where the "camel's-back line" is much broader.

Figure 6 shows the temperature dependence of the line shape of the camel's-back band for $T = 20$, 30, 40, and 50 K. With increasing temperature the structure due to the different phonons is smeared out and the lines broaden. The same effect can be achieved by increasing in an arbitrary way the carrier density by an appreciable amount, which increases the Fermi energy in the parabolic case as

$$E_F = (\hbar^2/2m^*)(3\pi^2 n)^{2/3} . \qquad (13)$$

This possibility was also studied and theoretical line shapes were calculated. These are not shown since it is considered that an arbitrarily large increase of the density is a less logical method for fitting the line shape. The calculated zero-field density is an upper bound for the actual density inside the drop at a finite temperature $T > 0$ K, since

$$n(T) = n_0[1 - \delta_n (kT)^2] , \qquad (14)$$

where δ_n is a thermal expansion coefficient, which is positive.[9]

V. COMPARISON OF EXPERIMENTAL AND THEORETICAL LINE SHAPES

The full line in Fig. 7 shows the experimental spectrum taken at 1.8 K and +20-nsec delay from the peak of the laser pulse (already given in Fig. 1). At this delay the (D^0,X) sulphur (or tellurium) line is weak (the N-bound exciton is even weaker) and its phonon replicas negligible[13,25] and so does not distort the line shape of the main band. The starting position for a comparison of the experimental and theoretical line shapes is therefore much better than hitherto.[6–8] This is mainly due to the excellent purity of the samples and to the analysis of spectra at short time delays when the impurity lines are weak (compare Fig. 2).

The main peak of the experimental curve in Fig. 7 is the LA(X) replica of the EHL recombination. At the low-energy side of this peak there is another band with $\simeq 10\%$ of the intensity of the main band. This band which is reported here for the first time is easily identified as arising from zone-center phonon replica of the main band. The peak positions of the replica TA(X), LA(X), and TO(X) + (LO(Γ), TO(Γ)) are indicated by arrows. These energies were derived by subtracting the appropriate phonon energies[13] from the energy of the main peak.

The dashed curve is a fit of the theoretical line shape for $T = 35$ K from Fig. 6 to the experimental one. There is excellent agreement between both lines close to the peak and to the lower- and higher-energy side up to about the half height of the

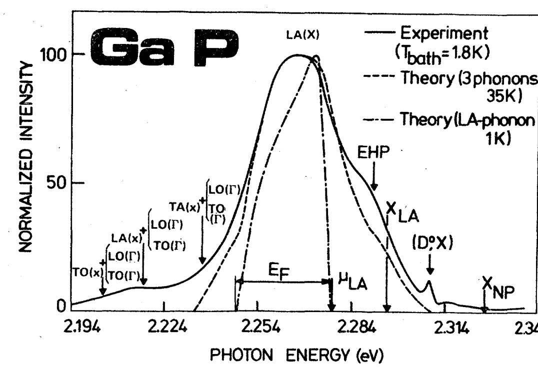

FIG. 7. Comparison of experimental and theoretical line shapes of the EHL. The straight line is an experimental curve for $T_{bath} = 1.8$ K at high excitation intensity ($\simeq 5$ MW/cm^2). (D^0,X) is the zero-phonon line of an exciton bound to a neutral S (or Te) donor. The dashed line is a fit to the $T = 35$ K theoretical curve of Fig. 6 and the dot-dashed line is the $T = 1$ K LA-phonon component of this line. μ is the chemical potential, X is the free-exciton energy gap (according to Ref. 14), E_F is the Fermi energy and TA, LA, LO, TO designate the different phonon replica.

peak. The slower decrease of the experimental line on the low-energy side can be explained by the presence of the multiphonon replica. It might also be partly due to Auger broadening.[57] No reliable intensity ratios of multiphonon replica of free carriers or free excitons are known to the authors in order to enable a discrimination to be made between these two possibilities.

At the high-energy side the experimental curve also falls more slowly than the theoretical one. It was mentioned earlier that the high-energy shoulder at $\simeq 2.29$ eV cannot be explained by the TA-phonon replica of the EHL and therefore it was concluded that the shoulder arises from emission from a lower-density plasma. There are two further independent pieces of evidence for this conclusion, which will be discussed now:

(i) It can be seen from Fig. 6 that the high-energy shoulder of the theoretical curves due to the TA replica disappears at 30 K ($\hat{=}2.6$ meV) due to thermal (or other) broadening mechanisms. There is theoretically no way to obtain a line shape that is similar to the experimentally measured one close to the peak and to retain at the same time the high-energy shoulder using the well-known phonon energies and intensities.

(ii) It was found that the *shoulder* became much less pronounced *and* shifted somewhat to lower energy after an increase of the excitation intensity at the highest densities applied, as shown in Fig. 8. This observation, which is similar to the change of the spectra at negative delay times (see Fig. 1), is inconsistent with a *pure* temperature broadening of an EHL line, although the peak shift is probably due to this effect. It should be emphasized that the main line shapes and peak positions at both excitation intensities are independent of delay time and so are characteristic of EHL's.

The observation can be understood, however, as a consequence of the existence of a plasma line at the high-energy side. With increase of the electron-hole density created by the laser the number of carriers in the liquid relative to the plasma, on phase separation, will increase (this is explained in more detail in Sec. VI; see Fig. 9). Thus a decrease in the plasma luminescence contribution relative to that of the liquid will be expected, in agreement with the experimental observation.

A slight increase in temperature might cause at the same time the density of the plasma which comes from the center of the excited region and which results from the phase separation to go up. This temperature increase shifts at the same time the EHL LA in Fig. 8 to higher energy—as predicted theoretically in Fig. 6—and causes a small low-energy shift of the plasma line. At much lower excitation intensity the plasma line could reach almost the height of the EHL line—however, the spectra were then strongly impurity distorted.

The dot-dashed line in Fig. 7 is the LA-phonon replica calculated for the same density, etc., as the three-phonon replica (dashed line) but for a temperature of 1 K. The relative positions of the two theoretical lines are, of course, fixed by theory and cannot vary. The high-energy onset of the LA line gives directly the energy position of the chemical potential μ_{LA} and the width of the line at the base gives the Fermi energy E_F. In a similar way one gets μ_{TO} and μ_{TA}.

The low-temperature threshold energies of the no-phonon exciton gap X_{NP} and of the LA(X) exciton gap ($X_{LA}=2.2955$ eV) as derived by Mobsby *et al.*[14] from a line-shape analysis of free-exciton luminescence lines are shown by arrows. The energy difference $X_{LA}-\mu_{LA}$ is 17.5 meV and is the binding energy of the EHL in GaP. This experimental value agrees well with the theoretical value of 14.0 meV. One might criticize the above approach

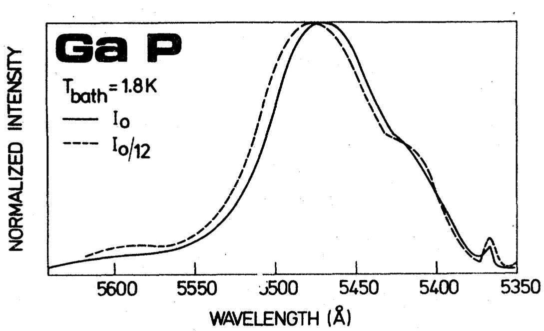

FIG. 8. Intensity dependence of the EHL line at two different intensities I_0 and $\frac{1}{12}I_0$ at $T_{bath}=1.8$ K. $I_0 \simeq 5$ MW/cm^2. The full line is the same as the experimental curve in Fig. 7.

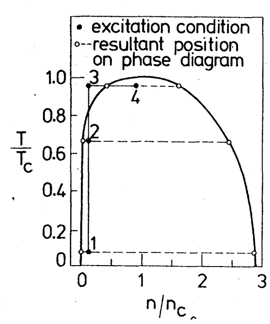

FIG. 9. Schematic universal phase diagram for gas-liquid coexistence. The line connecting the points 1–3 shows the result of an increase of the temperature on the decomposition into EHL and EHP. The line connecting points 3 and 4 gives the result of an increase of excitation intensity. This path illustrates in a graphical way the changes between the experimental spectra shown in Figs. 8, 10, and 11.

TABLE III. Comparison of the results of the line-shape fit made by different authors with the results of this paper. It should be noted that the density reported here was not used as a free parameter and fitted to the line shape; it is the theoretically determined value.

	Density (cm^{-3})	Experimental binding energy (meV)
This paper	8.6×10^{18}	17.5 ± 3
Maaref *et al.* (Ref. 6)	15.7×10^{18}	6.03
Shah *et al.* (Ref. 7)	6×10^{18}	14
Hulin *et al.* ($T=0$ K value) (Ref. 8)	15×10^{18}	8

on the grounds that it is incorrect to fit an experimental line shape at a finite temperature by a theoretical one using the calculated zero-temperature density (see Fig. 9 for the temperature dependence of the density). However, it is not claimed that the actual temperature of the EHL at a bath temperature of 1.8 K is 35 K. In contrast there is evidence that it is below 15 K, where the density is still $\simeq n_0$ (see Fig. 9). Even a slight increase of the density has a similar effect as the temperature in smearing out the phonon structure and helps to reduce the "fit temperature" drastically. Furthermore, there are at least two other broadening mechanisms that were not taken into consideration for the line-shape fit. The dispersion of the phonon energies was discussed in Sec. IV C. It is largest for the LA phonon and smallest for the TO phonon.[42] This dispersion gives rise to a broadening by $\simeq$3.5–4 meV of the dominating LA replica of the EHL and to a high-energy shift of the peak by $\simeq$2 meV, an effect also observed in bound-exciton spectra.[40] Second, electrons and holes with energies smaller than their respective Fermi energies create a final state of finite lifetime[58,59] after their recombination, since charge carriers with higher energies will relax to fill the empty states in the Fermi sea. This effect causes an inhomogeneous Lorentzian broadening of the line shape shown to be of importance for an accurate fit in Ge.[57] It should be of at least the same importance in GaP with its larger Fermi energies. Finally, there is the superposition of the EHP band. Under these circumstances it is rather difficult to estimate a proper temperature of the EHL. However we tend to assume—as is shown in Sec. VI—that the actual EHL temperature is not too far from the bath temperature and the observed broadening of the EHL line is due to the effects discussed above. This would justify the choice of density for the line-shape fit as being close to the zero-temperature density and would leave the temperature in the role of a meaningless variable that creates some broadening. Fits with different temperatures were tried but the resultant chemical potential did not deviate by more than $\simeq$3 meV from the value given where the effect of phonon dispersion was already included. Table III compares the binding energies determined in this paper with the values given in other recent publications.[6-8] The binding energy of the EHL in GaP found here is larger than any value reported hitherto.[6-8]

VI. CRITICAL TEMPERATURE OF THE PHASE TRANSITION

In this section evidence is presented that the critical temperature for EHL formation is close to 45 K. Using this temperature, we find excellent agreement with the thermodynamical scaling law which connects critical temperature and density.

Temperature-dependent spectra up to 100 K were measured. On increasing the temperature, no abrupt change of the shape of the luminescence band was observed. Instead the band shifted slightly to higher energy and broadened mainly on the high-energy side. The shift of the low-energy edge to higher energy with increasing temperature can be explained by the reduction of the EHL density with temperature. The broadening on the high-energy side is due to increase of the importance of the plasma line. The equidensity line $1\rightarrow2$ in Fig. 9 shows in a schematic way how these two phenomena occur.

The presence of an EHL was monitored in the same way as at low temperatures by taking time delayed spectra. In Fig. 10 such spectra taken for a temperature of 30 K and time delays $\Delta t=0$ and 100 nsec are shown. The low-energy edge, the peak, and the width of the luminescence band are again time independent, thus demonstrating that the EHL is still present at this temperature. The most striking difference compared to Fig. 1 is that in addition to a weak bound-exciton line being observed at long time delays the free exciton TO-, LA-, and TA- (not shown here) phonon

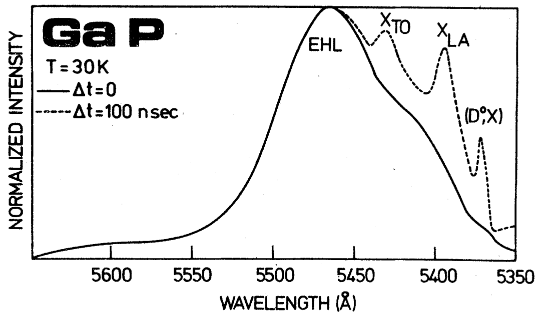

FIG. 10. Time-delayed spectra at $T_{\text{bath}} = 30$ K for time delays $\Delta t = 0$ and 100 nsec relative to the maximum of the emission. $X_{\text{TO,LA}}$ are the TO(X) and LA(X) replicas of the free exciton. (D^0,X) is the sulphur- (tellurium-) bound exciton.

replica were observed. The temperature dependence of the excitonic lines is very similar to that found under conditions of much less intense cw pumping[14] thus indicating that under the present intense pulsed laser conditions the lattice temperature at least is reasonably close to the bath temperature. Using the same excitation intensity the existence of an EHL at 40 K could not be proved. Apparently the step from 2 to 3 in the sketch of Fig. 9 is made: the border line of the phase transition is crossed. However, by increasing the intensity by a factor of 4 and thereby going from 3 to 4 in Fig. 9 the EHL was again created. Figure 11 shows the strong low-energy shift of the line after this intensity increase. The same procedure was not possible at 50 K (the surface of the crystal was damaged after further increase of the excitation intensity). The lower limit of T_c is therefore ~45± 5 K. T_c is not believed to be higher than 50 K.

Hensel *et al.* have compared in their review[9] the critical parameters n_c, T_c of the phase diagram for Si and Ge and found for these two materials

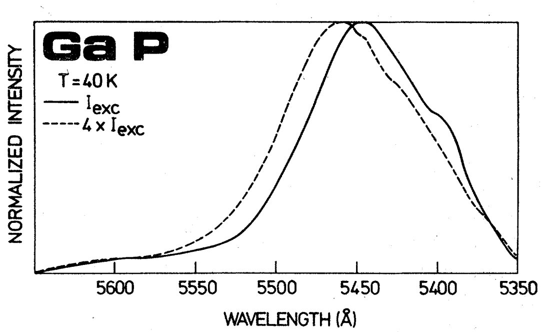

FIG. 11. Two luminescence spectra taken at an excitation intensity of ~ 5 and 20 MW/cm^2 at a temperature of the surrounding He gas of 40 K.

TABLE IV. Critical temperature T_c, zero-temperature density n_0, and constant $\beta = \sqrt{n_0}/T_c$ for four semiconductors that show a phase transition to an EHL.

	T_c (K)	n_0 (cm^{-3})	$\beta = \sqrt{n_0}/T_c$ (cm$^{-3/2}$ K^{-1})
Ge	7[a]	2.45×10^{17} [b]	7.1×10^7
Si	25[c]	3.3×10^{18} [c]	7.3×10^7
SiC	41[d]	9.2×10^{18} [e]	7.4×10^7
GaP	45[f]	8.6×10^{18} [f]	6.5×10^7

[a]Reference 60.
[b]Reference 61, model HA II.
[c]Reference 62.
[d]Reference 2.
[e]Reference 63.
[f]This paper.

$$n_c(\text{Si})/n_c(\text{Ge}) \sim \xi\,, \tag{15a}$$

$$T_c(\text{Si})/T_c(\text{Ge}) \sim \xi^{1/2}\,. \tag{15b}$$

This observation can be reformulated as a scaling rule

$$n_c^{1/2}/T_c = \text{const} \tag{16}$$

and it is interesting to test whether it applies to other materials than just Si and Ge, for which the agreement of the constants in Eqs. (15a) and (15b) might be fortuitous. It is already rather difficult, however, to determine n_c for Ge and Si, and the numbers obtained are not very precise. On the other hand it is easy to verify Eq. 15 also holds for the density at zero temperature n_0.

Table IV lists the values of the critical temperatures T_c and zero temperature densities for Ge, Si, SiC, and GaP and compares

$$n_0^{1/2}/T_c = \beta\,. \tag{17}$$

Here we have assumed T_c(GaP) = 45 K. The scaling law [Eq. (17)] is well obeyed by all four different materials, a demonstration that it indeed has a general character. At the same time the result for β adds weight to the present value for T_c, which is in good agreement with the value of Shah *et al.*[7]

VII. CONCLUSION

An investigation of the luminescence of high-purity epitaxial GaP under conditions of high excitation (I_{exc}~ 10 MW/cm^2) and as a function of the excitation intensity, the temperature, and the time after excitation has been presented. Evidence was given from time-delayed spectra that at temperatures $T_c \lesssim 45$ K a phase transition from an electron-hole plasma (EHP) to an electron-hole liquid (EHL) occurs. The prominent luminescence band detected in the region of 2.26 eV was proved to be composed of recombination radiation originating from both the EHL and the EHP, a fact that was found to be decisive for a quantitative understanding of the experimental results.

The ground-state properties of the EHL were calculated, including the effect of the camel's-back-like conduction-band minimum. It was shown to be more important than the electron-phonon interaction correction to the exchange and yielded a ground-state energy of 33.3 meV, a binding energy of 14 meV, and a density of 8.6×10^{18} cm^{-3}. An independent determination of $E_B^{\cdot}$ from a line-shape fit yields the value 17.5 meV. The high density of states of the camel's back is also shown to influence very strongly the ratio of the electron and hole Fermi energies of the EHL, leading to a value of $E_F^h/E_F^e \simeq 4.9$, which should give rise to a strong charging of the drops in GaP. Following a suggestion by Hensel *et al.* a universal scaling law relating the critical temperature T_c and the low-temperature density n_0 is firmly established for the four best-known materials that exhibit this electronic phase transition and the constant $\beta = n_0^{1/2}/T_c$ is given to be $(7.0\pm0.5)\times10^7$ cm$^{-3/2}$K^{-1}.

ACKNOWLEDGMENTS

We are very indebted to P. J. Dean and U. Rössler for various comments and for a critical reading of the manuscript. We are also very grateful to R. G. Humphreys for allowing us to quote his results on the depth of the camel's back prior to publication and for many helpful discussions about all aspects of the camel's back. K. Dransfeld, G. Landwehr, and H. J. Queisser encouraged this work considerably by their continuous interest. We would like to thank C. Weyrich and D. R. Wight for the gift of the samples, H. Krath for his valuable help with the experiments, and R. Baumert for experimental spectra he kindly took at an early stage of this work. One of us (L.M.S.) would like to thank the Max-Planck-Institut, Grenoble, for hospitality during the period when this work was performed and to the NSF for partial support.

---

*Present address: Max Planck Institut für Festkörperforschung, Heisenberg Str. 1, 7 Stuttgart, Germany.

†Present address: RSRE, St. Andrews Road, Great Malvern/Worcestershire, England.

[1]H. R. Trebin and U. Rössler [Phys. Status Solidi B 70, 717 (1975)] calculate the hole-phonon coupling. The electron-phonon coupling α can be calculated using the well-known formula

$$\alpha = \frac{e^2}{2\hbar\omega_{\rm LO}}\left(\frac{2m^*\omega_{\rm LO}}{\hbar}\right)^{1/2}\left(\frac{1}{\epsilon_\infty}-\frac{1}{\epsilon_0}\right).$$

[2]D. Bimberg, M. S. Skolnick, and W. J. Choyke, Phys. Rev. Lett. 40, 56 (1978).

[3]F.H. Pollak, C. W. Higginbotham, and M. Cardona, J. Phys. Soc. Jpn. Suppl. 21, 20 (1966).

[4]P. Lawaetz, Solid State Commun. 16, 65 (1975).

[5]P. J. Dean and D. C. Herbert, J. Lumin. 14, 55 (1976).

[6]H. Maaref, J. Barrau, M. Brousseau, J. Collet, and J. Mazzaschi, Solid State Commun. 22, 593 (1977).

[7]J. Shah, R. F. Leheny, W. R. Harding, and D. R. Wight, Phys. Rev. Lett. 38, 1164 (1977).

[8]D. Hulin, M. Combescot, N. Bontemps, and A. Mysyrowicz, Phys. Lett. A 61, 349 (1977).

[9]See, e.g., the reviews by J. C. Hensel, T. G. Phillips, and G. A. Thomas, *Solid State Physics*, edited by F. Seitz, D. Turnbull, and H. Ehrenreich (Academic, New York, 1977); M. Voos and C. Benoît à la Guillaume, *Optical Properties of Solids, New Developments*, edited by B. O. Seraphin (North Holland, Amsterdam, 1976), p. 145; Ya. E. Pokrovskii, Phys. Status Solidi A 11, 385 (1972).

[10]G. Beni and T. M. Rice, Solid State Commun. 23, 871 (1977).

[11]P. Vashishta, S. G. Das, R. K. Kalia, and D. S. Singwi, Bull. Am. Phys. Soc. 22, 269 (1977).

[12]D. G. Thomas and J. J. Hopfield, Phys. Rev. 150, 680 (1966).

[13]D. G. Thomas, M. Gershenzon, and J. J. Hopfield, Phys. Rev. 131, 2397 (1961); P. J. Dean, *ibid.* 157, 655 (1967).

[14]C. D. Mobsby, E. C. Lightowlers, and G. Davies, J. Lumin. 4, 29 (1971).

[15]A. Onton, Phys. Rev. B 4, 4449 (1971).

[16]See, for example, Y. Couder, M. Hulin, and H. Thomé, Phys. Rev. B 7, 4373 (1973); M. von Ortenberg and K. J. Button, *ibid.* 16, 2618 (1977).

[17]J. C. Hensel and E. O. Kane (private communication).

[18]P. J. Dean and D. G. Thomas, Phys. Rev. 150, 690 (1966).

[19]A. N. Pikhtin and D. A. Yas'kov, Sov. Phys. Solid State 11, 455 (1969).

[20]Taken from data compiled by D. E. Hill.

[21]R. G. Humphreys, U. Rössler, and M. Cardona, Phys. Rev. B 18, 5590 (1978).

[22]M. Capizzi, F. Evangelisti, P. Fiorini, A. Frova, and F. Patella, Solid State Commun. 24, 801 (1977).

[23]M. Altarelli, R. A. Sabatini and N. O. Lipari, Solid State Commun. 25, 1101 (1978).

[24]A. A. Kopylov and A. N. Pikhtin, Fiz. Tech. Poluprov. 11, 867 (1977) [Sov. Phys. Semicond. 11, 510 (1977)].

[25]P. J. Dean, D. Bimberg, and F. Mansfield, Phys. Rev. B 15, 3906 (1977).

[26]A. C. Carter, P. J. Dean, M. S. Skolnick, and R. A. Stradling, J. Phys. C 10, 5111 (1977).

[27]D. O. Manchon and P. J. Dean, *Proceedings of the Tenth International Conference on the Physics of Semiconductors, Cambridge, 1970* (U.S. AEC, Oak Ridge, 1970), p. 760.

[28]J. Leotin, J. C. Ousset, R. Barbaste, S. Askenazy, M. S. Skolnick, R. A. Stradling, and G. Poiblaud, Solid State Commun. 16, 363 (1975).

[29]K. Suzuki and N. Miura, Solid State Commun. 18, 233 (1976).

[30]A. T. Vink, R. A. van der Heyden, and J. A. W. van der Does de Bye, J. Lumin. 8, 105 (1973).

[31]R. A. Street and W. Senske, Phys. Rev. Lett. 37, 1292 (1976).

[32]The interpretation of Street and Senske's experiments was recently doubted by M. D. Sturge, A. T. Vink, and F. J. M. Kuujpers [Appl. Phys. Lett. 32, 49 (1977)]. However, the modification in E_A proposed there did not make it easier to assign some unexplained transitions in the spectra of Ref. 31.

[33]A. Baldereschi and N. O. Lipari, Phys. Rev. B 9, 1525 (1974).

[34]W. Senske (private communication). The anisotropy γ_2/γ_3 might be still somewhat overestimated as discussed by D. Bimberg and P. J. Dean, Phys. Rev. B 15, 3917 (1977), due to an underestimate of γ_2.

[35]J. Leotin, R. Barbaste, S. Askenazy, M. S. Skolnick, R. A. Stradling, and J. Tuchendler, Solid State Commun. 15, 693 (1974).

[36]H. J. Zeiger, B. Lax, and R. N. Dexter, Phys. Rev. 105, 495 (1957). For Ge, Si, and GaAs this value is in excellent agreement with that found in Ref. 43.

[37]M. Combescot and P. Nozières, J. Phys. C 5, 2369 (1972).

[38]D. Auvergne, P. Merle, and H. Mathieu, Phys. Rev. B 12, 1371 (1975).

[39]D. R. Wight, J. Phys. C 1, 1759 (1968).

[40]P. J. Dean, R. A. Faulkner, and S. Kimura, Phys. Rev. B 2, 4062 (1970).

[41]G. A. Thomas and M. Capizzi, *Proceedings of the Thirteenth International Conference on the Physics of Semiconductors, Rome, 1976*, edited by G. Fumi (Marves, Rome, 1976), p. 914.

[42]J. L. Yarnell, J. L. Warren, R. G. Wenzel, and P. J. Dean, *Neutron Elastic Scattering* (International Atomic Energy Agency, Vienna, 1968), p. 301.

[43]W. F. Brinkman and T. M. Rice, Phys. Rev. B 7, 1508 (1973).

[44]H. L. Störmer, R. W. Martin, and J. C. Hensel, in Ref. 41, p. 950.

[45]H. Büttner, *Proceedings of the Twelfth International Conference on the Physics of Semiconductors, Stuttgart, 1974*, edited by M. H. Pilkuhn (Teubner, Stuttgart, 1974), p. 81.

[46]C. Benoît à la Guillaume (private communication).

[47]P. Vashishta, P. Bhattacharyya, and K. S. Singwi, Nuovo Cimento B 23, 172 (1974); Phys. Rev. B 10, 5108 (1974).

[48]G. Beni and T. M. Rice, Phys. Rev. Lett. 37, 874 (1976).

[49]L. V. Keldysh and A. P. Silin, Zh. Eksp. Teor. Fiz. 69, 1053 (1975) [Sov. Phys. JETP 42, 535 (1976)].

[50]N. O. Lipari (private communication) calculates $E(\frac{3}{2}) = 18.5$ meV and $E(\frac{1}{2}) = 19.3$ meV for the parameters used here. The splitting of the two states of 0.8 meV is too small as compared to the experimental result of Humphreys *et al.* (Ref. 21) indicating that γ_2 might be actually somewhat larger (see Ref. 34).

[51]R. Bindemann, R. Schwabe and T. Hänsel, Phys. Status Solidi B 87, 169 (1978).

[52]T. M. Rice, Phys. Rev. B 9, 1540 (1974).

[53]T. L. Reinecke and S. C. Ying, Solid State Commun. 14, 381 (1974).

[54]P. Vashishta, S. G. Das, and K. S. Singwi, Phys. Rev. Lett. 33, 911 (1974).

[55]R. K. Kalia and P. Vashishta, Solid State Commun. 24, 171 (1977).

[56]J. H. Rose and H. B. Shore (unpublished).

[57]R. W. Martin and H. L. Störmer, Solid State Commun. 22, 523 (1977).

[58]P. T. Landsberg, Proc. Phys. Soc. A 62, 806 (1949).

[59]P. T. Landsberg, Phys. Status Solidi 15, 623 (1966).

[60]W. Miniscalco, C.-C. Huang, and M. B. Salamon, Phys. Rev. Lett. 39, 1356 (1977).

[61]P. Bhattacharyya, V. Massida, K. S. Singwi, and P. Vashishta, Phys. Rev. B 10, 5127 (1974).

[62]R. B. Hammond, T. C. McGill, and J. W. Mayer; Phys. Rev. B 13, 3566 (1976).

[63]D. Bimberg, L. M. Sander, M. S. Skolnick, U. Rössler, and W. J. Choyke, J. Lumin. (to be published).

[64]M. Cardona, J. Phys. Chem. Solids 24, 1543 (1963).